# A critical-state constitutive model for rate-dependent deformation of permafrost


Dana Amini [(1)], Pooneh Maghoul [(2,1)], Hartmut Hollaender [(1)]
*(1) Department of Civil Engineering, University of Manitoba, Winnipeg, Manitoba, Canada*
*(2) Department of Civil, Geological and Mining Engineering, Polytechnique Montréal, Montréal, Quebec, Canada*

ABSTRACT
In permafrost regions, the long-term serviceability of infrastructure founded on highly plastic foundation is adversely affected by slow-rate, time-dependent deformations (i.e., viscous or creep behavior) of permafrost subject to climate change. Investigating such deformations in a Thermo-Hydro-Mechanical (THM) framework requires a coupled non-isothermal strain-rate geomechanical constitutive model. Long-term deformations of geomaterials are commonly estimated by a combination of instant and delayed components of deformations. The instant component is associated with largely reversible (elastic) deformations of the soil while the delayed component includes non-recoverable (plastic), time-dependent and simultaneous thermo-viscoplastic reorganization of the inter-particle microstructure. Based on this approach, a Thermal Elastic-ViscoPlastic (TEVP) constitutive model is formulated in accordance with the Critical State Soil Mechanics (CSSM) framework to investigate the creep behavior of permafrost. The model predictions fit reasonably well the experimental data available in the literature.

RÉSUMÉ
Dans les régions nordiques, la performance à long terme des infrastructures fondées sur des sols de plasticité élevée est affectée par les déformations lentes et dépendantes du temps (c.-à-d. comportement visqueux ou de fluage) du pergélisol soumis aux changements climatiques. L'étude de ces déformations dans un cadre thermo-hydro-mécanique (THM) nécessite un modèle de comportement géomécanique couplé non isotherme dépendant de la vitesse de déformation. Les déformations à long terme des géomatériaux sont généralement estimées par une combinaison de composantes instantanées et tardives des déformations. La composante instantanée est associée à des déformations largement réversibles (élastiques) du sol tandis que la composante tardive comprend une réorganisation simultanée thermo-viscoplastique non récupérable (plastique) de la microstructure inter-particules dépendante du temps. Sur la base de cette approche, un modèle constitutif thermique élastique-viscoplastique (TEVP) est formulé conformément au cadre de la mécanique des sols à l'état critique (CSSM) pour étudier le comportement de fluage du pergélisol. Les prédictions du modèle correspondent raisonnablement bien aux données expérimentales disponibles sur le comportement dépendant du temps et de la température des échantillons gelés.

## 1 INTRODUCTION

Permafrost, known as the ground that remains at or below 0 ºC for at least two consecutive years, underlies a large portion of the land surface in the northern hemisphere. Such sub-zero temperatures ensure the presence of ice-inclusion geomaterials in Arctic and sub-Arctic regions. The soil-atmosphere interactions, in the context of climate change, result in short- and long-term changes in permafrost thermal conditions. Rates of change in temperature are not identical spatially and temporally. For instance, the abrupt changes in permafrost thermal conditions can be caused by seasonal weather as well as the appearance of extreme climatic events during the cold and warm seasons. Such different rates of thermal loading lead to the spatio-temporal change of permafrost landscape and behavior in northern regions.

In permafrost regions, the existence of ice in the ground increases the mechanical strength of the ground by producing an apparent cohesion. In warm permafrost regions, the melting of ice inclusion in the ground generates unfrozen water and excess pore water pressure under sufficiently fast thawing rates. Upon melting, the strength of the ground reduces due to the disappearance of ice bonding. It causes ground surface deformations, strength loss, and permafrost degradation, which consequently endanger the integrity and serviceability of infrastructure in permafrost regions. It is proven that the magnitude of such deformations predominantly depends on the permafrost type, amount of ground ice, and temperature. Coastal erosion and abrupt thaw slump events are known as typical permafrost degradation in ice-rich permafrost regions (e.g., Teufel and Sushama 2019).

The coexistence of ice and unfrozen water also causes irrecoverable slow-rate time-dependent deformation (i.e., creep behavior) of permafrost under prolonged constant stress conditions. It is usually assumed that creep deformation (also referred to as secondary compression) either starts simultaneously with the primary (instant) deformation or occurs after the end of that. In addition to the primary and secondary deformations, tertiary creep deformation is also observed in ice-rich permafrost that can result in accelerated deformation of infrastructure founded on highly plastic permafrost (Andersland and Ladanyi

2003). Temperature, confining stress level, strain rate, ice content, and ground stratigraphy are known as factors controlling the rheological properties and the stages of the creep curve for most frozen soils (Andersland and Ladanyi 2003).

To date, many experimental attempts have been made to capture the impacts of the aforementioned controlling parameters on the creep behavior of frozen soils (e.g., Vyalov 1986; Arenson and Springman 2005a; Yao et al. 2018). Moreover, in the geotechnical context, various constitutive models have been developed to theoretically examine the creep behavior of frozen soils. A few creep models based on the theory of elastic-visco-plasticity or visco-elastic-plasticity have been developed for frozen soils by considering the effects of time and temperature rates. Due to the close analogy between frozen soils and unsaturated soils, an elastic-viscoplastic model based on the framework of two-stress-state variables was proposed by Ghoreishian Amiri et al. (2016a) to describe the rate-dependent behavior of frozen soils. In this model, viscoplastic strains are incorporated into the formulation in accordance with the overstress theory proposed by Perzyna (1963). Sun et al. (2021) proposed a theoretical poro-visco-elastic-plastic damage model that accounts for creep behavior and anisotropic damage behavior of saturated frozen soils. Assuming frozen soil as a viscoelastic material, Li et al. (2022) have proposed a viscoelastic-plastic constitutive model for frozen soil, disregarding the time-dependent development of plastic strains.

More extensive knowledge of the impacts of ground ice, rate of thermal state change, mechanical stress levels, and their inter-dependencies are still required to investigate the rate-dependent behavior of permafrost. This calls for an advanced constitutive model that captures the thermal creep deformations and the creep-induced shear failure of frozen soils. In this paper, a thermal elastic–viscoplastic (TEVP) geomechanical constitutive model is developed based on the Critical State Soil Mechanics (CSSM) to investigate the rate-dependency behavior of frozen soils. In order to demonstrate the capability of the model to properly capture the time- and temperature-dependent behavior of frozen soils, the model predictions are compared with experimental test results in the literature.

## 2 FROZEN SOILS – BASIC CONCEPTS AND STRESS STATE VARIABLES

From a poromechanical point of view, a frozen soil is a medium composed of a deformable solid skeleton and a porous space filled with unfrozen water and ice. The volumetric fractions of the solid skeleton, $\theta_s$, unfrozen water, $\theta_w$, and ice content, $\theta_i$, can be described as follows:

$$\theta_s = 1 - n,\ \ \theta_w = nS_w,\ \ \theta_i = nS_i,\ \ S_w + S_i = 1 \qquad [1]$$

where $n = \theta_w + \theta_i$ is the porosity that increases with freezing in-situ pore-water; $S_w$ and $S_i$ are the degrees of saturation relative to water and ice, respectively.

In order to describe the behavior of frozen soils, the effect of the cryogenic suction change on the skeleton deformation is required to be incorporated into the formulation. Considering the ice crystals as a part of the solid phase, the formulation of the constitutive model can be presented within the framework of two-stress state variables in which the cryogenic suction defined as:

$$S = P_{ice} - P_w \qquad [2]$$

and the solid phase stress proposed by Ghoreishian Amiri et al. (2016b) as:

$$\boldsymbol{\sigma}^* = \boldsymbol{\sigma} - S_w P_w \boldsymbol{I} \qquad [3]$$

are the stress state variables. In Eq. 2, $S$ is the cryogenic suction; $P_{ice}$ and $P_w$ denote the pressure of ice and water phases, respectively. $\boldsymbol{\sigma}^* (= \sigma_{ij}^*)$ stands for the solid phase stress tensor; $\boldsymbol{\sigma}$ $(= \sigma_{ij})$ denotes the total stress tensor; $\boldsymbol{I}$ $(= I_{ij})$ is the second-order isotropic tensor with component $\delta_{ij}$, where $\delta_{ij}$ is the Kronecker delta. The cryogenic suction can be approximated by the thermodynamic equilibrium at the ice-water interface described by the Clausius–Clapeyron equation as follows:

$$S \approx \rho_w L \ln\left(\frac{T}{273.15}\right) \qquad [4]$$

where $\rho_w$ stands for the density of unfrozen water (1000 kg/m$^3$), $L$ is the latent heat of freezing due to the phase change of water ($334\times10^3$ J/kg), and $T$ indicates temperature (Kelvin). Eq. 4 denotes that the variation of cryogenic suction can be estimated by the variation of temperature.

## 3 THERMAL ELASTIC–VISCOPLASTIC (TEVP) MODEL

In order to formulate the behavior of frozen soils, two constitutive laws are required to address the effect of cryogenic suction (or temperature) on deformation and (unfrozen water) saturation; the former is the stress-suction-strain relation to consider the effect of cryogenic suction on the strain. The latter is the suction-saturation relation to describe the evolution of saturation under the variation of cryogenic suction. The first constitutive law of the skeleton relates the solid phase stress increments with strain increments considering the effect of cryogenic suction. For this purpose, the total strain rate can be decomposed into two mechanical (solid phase stress-dependent) and cryogenic suction-dependent components. It is assumed that the strain rate due to changes in solid phase stress is separated into elastic (time-independent recoverable) and thermal-viscoplastic (time- and temperature-dependent irrecoverable) components. Therefore, the total strain can be written as follows:

$$\dot{\boldsymbol{\varepsilon}} = \dot{\boldsymbol{\varepsilon}}^{\sigma} + \dot{\boldsymbol{\varepsilon}}^{suc} = (\dot{\boldsymbol{\varepsilon}}^{\sigma e} + \dot{\boldsymbol{\varepsilon}}^{\sigma Tvp}) + \dot{\boldsymbol{\varepsilon}}^{suc} \qquad [5]$$

where $\dot{\boldsymbol{\varepsilon}}$ $(= \dot{\varepsilon}_{ij})$ is the second-order total strain rate tensor and the over-dot indicates the time rate of change ($\dot{\varepsilon}_{ij} = \delta\varepsilon_{ij}/\delta t$, where $t$ is the time); $\dot{\boldsymbol{\varepsilon}}^{\sigma}$ and $\dot{\boldsymbol{\varepsilon}}^{suc}$ are the strain rate due to the solid phase stress changes and suction changes, respectively; $\dot{\boldsymbol{\varepsilon}}^{\sigma e}$ and $\dot{\boldsymbol{\varepsilon}}^{\sigma Tvp}$ are the elastic and thermo-visco-plastic components of strain rate due to changes in stress, respectively.

The model can be partitioned into volumetric and deviatoric stresses and strains. The mean solid phase stress ($p^*$) and deviatoric stress ($q^*$) are defined as

$$p^* = \sigma_{ii}^*/3 = (\sigma_{11}^* + \sigma_{22}^* + \sigma_{33}^*)/3 \quad [6]$$

and

$$q^* = \sqrt{3 s_{ij}^* s_{ij}^*/2} \quad [7]$$

where $s_{ij}^*$ is the deviatoric solid phase stress tensor with components $(\sigma_{ij}^* - p^* \delta_{ij})$, $\sigma_{ij}^*$ is the solid phase stress tensor defined earlier.

### 3.1 Elasticity

Elastic volumetric strain rates are considered to be composed of two separate solid phase stress- and cryogenic suction-induced components ($\dot{\varepsilon}_p^e = \dot{\varepsilon}_p^{\sigma e} + \dot{\varepsilon}_p^{suc}$). It is assumed that the elastic shear strain rate is purely mechanical, with no cryogenic suction related component ($\dot{\varepsilon}_q^e = \dot{\varepsilon}_q^{\sigma e}$).

The elastic component of strain rate tensor due to the solid phase stress variation can be written as

$$\dot{\varepsilon}_{ij}^{\sigma e} = \frac{\dot{p}^*}{3K_{eq}} \delta_{ij} + \frac{1}{2G_{eq}} \dot{s}_{ij}^* \quad [8]$$

where $G_{eq}$ and $K_{eq}$ are temperature- (or suction-) dependent equivalent shear modulus and bulk modulus of the mixture. Given the assumption of the ice crystals as a part of the solid phase, the equivalent elastic parameters of the mixture depend on ice saturation as follows (Ghoreishian Amiri et al. (2016b)):

$$G_{eq} = (1 - S_i) G_{uf} + S_i \frac{E_f}{2(1+\nu_f)} \quad [9]$$

and

$$K_{eq} = (1 - S_i) K_{uf} + S_i \frac{E_f}{3(1-2\nu_f)} \quad [10]$$

where $G_{uf}$ and $K_{uf}$ are, respectively, the shear modulus and bulk modulus of the soil in an unfrozen state; $\nu_f$ and $E_f$ are Poisson's ratio and Young's modulus (i.e., deformation parameters) of the soil in the fully frozen state. The deformation parameters of a frozen soil depend on soil type and its temperature (Andersland and Ladanyi 2003). It is experimentally demonstrated that Young's modulus of frozen soils increases with decreasing temperature. Different empirical equations are presented in the literature to express the variation of Young's modulus with temperature. In the present study, the following empirical expression is employed for $E_f$:

$$E_f = E_{uf}(1 + a\theta) \quad [11]$$

where $E_{uf}$ is Young's modulus of the soil in an unfrozen state; $a$ is a material parameter denoting the change in $E_f$ with temperature; and $\theta$ is the absolute number of sub-zero ºC temperature.

The strain due to cryogenic suction changes (i.e., $\delta \boldsymbol{\varepsilon}^{suc} = \dot{\boldsymbol{\varepsilon}}^{suc} \times \delta t$) is assumed to be elastic and volumetric. This assumption is by disregarding the creation of ice lenses. This can be interpreted by the curvature-induced premelting mechanism within the theory of premelting dynamics (Rempel et al. 2004). This mechanism is closely the same as the capillary suction mechanism in unsaturated soils. Hence, the same expression as the one proposed for unsaturated soils (e.g., Alonso et al. 1990), can be adopted to determine the volumetric elastic part of the strain due to suction variation. Thus,

$$\delta \boldsymbol{\varepsilon}^{suc} = (\boldsymbol{D}^{suc})^{-1} \delta S \quad [12]$$

where $\delta S$ denotes cryogenic suction changes and $\boldsymbol{D}^{suc}$ is the elastic cryogenic suction–strain tensor that can be expressed as:

$$(\boldsymbol{D}^{suc})^{-1} = \frac{1}{3V} \frac{\kappa_s}{(S + P_{atm})} \boldsymbol{I} \quad [13]$$

where $\kappa_s$ is the elastic stiffness parameter for changes in cryogenic suction; $V$ is the specific volume; and $P_{atm}$ is the atmospheric pressure.

### 3.2 Viscoplasticity

#### 3.2.1. Behavior of Frozen Soil in $q^* - p^* - S$ space

The freezing process in soils is accompanied by an increase in mechanical strength. This is because of the formation of pore ice at below zero temperatures. Upon thawing, the loss of soil strength occurs due to the melting of the pore ice, resulting in subsequent settlements. Therefore, a suction-dependent criterion is required to capture the essential features of frozen and unfrozen behavior. Given the close analogy between the suction-dependent stress-strain behavior of frozen soils and unsaturated soils, the yield surface or plastic potential surface in the Barcelona Basic Model (BBM) proposed by Alonso et al. (1990) for unsaturated soils is adopted in the TEVP constitutive model presented in this study to formulate the behavior of frozen soils. Hence, considering the solid phase stress and cryogenic suction as the two stress state variables, this suction-dependent surface can be expressed in the $q^* - p^* - S$ space as follows:

$$F = q^{*2} - M^2 (p^* - p_t^*)(p_f^* - p^*) = 0 \quad [14]$$

where $p_t^*$ $(= -k_t S)$ denotes the apparent cohesion of the frozen soil due to cryogenic suction ($k_t$ is the parameter denoting the increase in apparent cohesion with cryogenic suction); $M$ is the slope of the critical state line (CSL) in $q^* - p^*$ space; and

$$p_f^* = p_r^* \left(\frac{p_o^*}{p_r^*}\right)^{\frac{\lambda_o - \kappa_o}{\lambda_f - \kappa_f}} \quad [15]$$

in which $p_o^*$ is the pre-consolidation stress in an unfrozen state, $p_r^*$ is the reference stress; $\kappa$ describes the compressibility coefficient within the elastic region that is assumed to be temperature- (or cryogenic suction-) independent $(\kappa_f = \kappa_o)$; $\lambda_f$ is the elastoplastic

compressibility coefficient of the soil in a frozen state. As proposed by Alonso et al. (1990) for unsaturated soils, for a frozen state of the soil, $\lambda_f$ can be correlated with the elastoplastic compressibility coefficient of the soil in an unfrozen state ($\lambda_o$) as follows:

$$\lambda_f = \lambda_o \left[(1-\alpha)\exp(-\beta S) + \alpha\right] \quad [16]$$

$\alpha$ is a model parameter related to the maximum stiffness of the soil and $\beta$ is a parameter that controls the rate of change in soil stiffness with cryogenic suction. A schematic of this surface is illustrated in Figure 1. Similar forms are also employed by other researchers for constitutive modeling of frozen soils (e.g., Nishimura et al. 2009; Ghoreishian Amiri et al. 2016a,b). As shown in this figure, in an unfrozen state (zero cryogenic suction), the surface reduces to that in the well-known Modified Cam-Clay model.

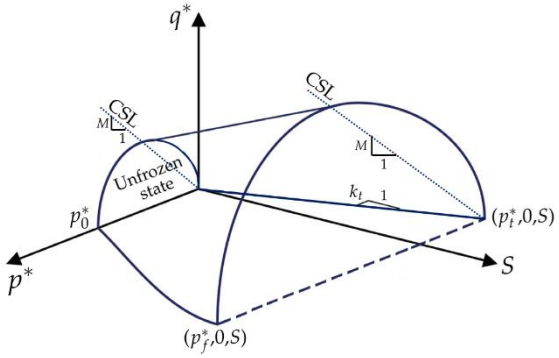


Figure 1. Illustration of the surface adopted for the TEVP constitutive modeling of frozen soils in $q^* - p^* - S$ space.

### 3.2.2. Thermal Viscoplastic Strains

In order to determine the suction- (or temperature-) dependent viscoplastic deformation, plastic potential and yield surfaces should be described at the current stress state of the soil ($q^* - p^* - S_1$). Therefore, the suction-dependent surface presented in Eq. 14 is adopted as the plastic potential surface (PPS) passing through the current stress state of frozen soil. The yield surface, inside which deformations are purely thermal elastic, can be described according to the current stress state and keep a similar shape to the PPS (see Figure 2). The current stress state remains outside the yield surface allowing the thermal plastic deformation of the soil with time (i.e., thermo-visco-plastic deformation).

It can be reasonably assumed that the plastic volumetric strain increment at the current stress state (see A in Figure 2) is equal to that under the corresponding isotropic stress state ($(q^* = 0) - (p^* = p_m^*) - S_1$), (see AA in Figure 2) (Tavenas et al. 1978). Therefore, thermal viscoplastic deformation is formulated by considering the response of frozen soil in isotropic compression. For this purpose, the changes in specific volume of frozen soil ($V$) under isotropic compression loading condition is investigated. As shown in Figure 2, in such loading conditions, combinations of the mean solid phase stress ($p_m^*$) and specific volume ($V_m$) form the isotropic normal compression line (NCL) at the current frozen state ($S = S_1$) of the soil in $p^* - V$ plane. According to the CSSM, the NCL can be expressed as:

$$V_{NCL} = N_f - \lambda_f \ln p_m^* \quad [17]$$

where $V_{NCL}$ is the specific volume of the frozen soil under isotropic compression of $p_m^*$, that can also be referred to as the specific volume of the frozen soil at the end of primary volumetric compression; $\lambda_f$ is the slope of the NCL (defined in Eq. 16) and $N_f$ is the specific volume at unit pressure in the current frozen state expressed as:

$$N_f = N_o + \kappa_s \ln \frac{S + P_{atm}}{P_{atm}} \quad [18]$$

where $N_o$ is the specific volume at unit pressure in an unfrozen state.

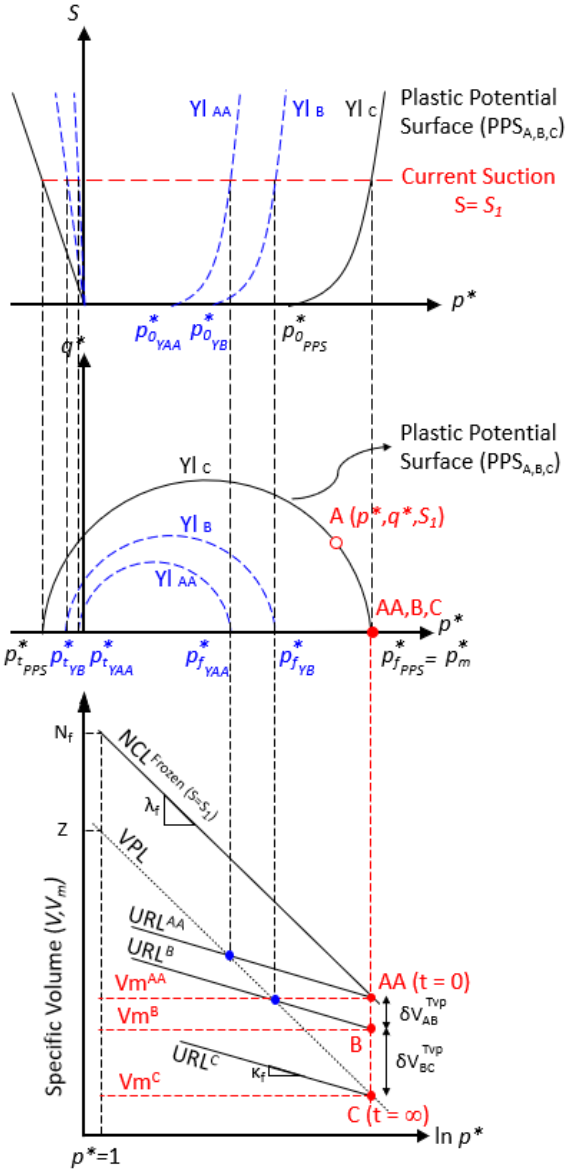


Figure 2. Description of the TEVP model and its parameters in $p^* - S$, $p^* - q^*$ and $\ln p^* - V$ planes.

Adopting a logarithmic creep function for frozen soils, the same as the one proposed by Yin and Graham (1999) for unfrozen soils, the purely time-dependent irrecoverable (i.e., viscoplastic) changes in the specific volume of frozen soil under the isotropic constant stress of $p_m^*$ corresponding to the current stress state of the soil can be formulated as follows:

$$\delta V_m^{\sigma Tvp} = -\psi_T \ln\left(\frac{t_o+t}{t_o}\right) \quad [19]$$

where $\delta V_m^{\sigma Tvp}$ is the thermal volumetric deformation of the frozen soil at time $t$ after the end of primary compression; $t_o$ is a material parameter denoting the initiation time of purely creep compression deformations, known as secondary creep. $\psi_T = \psi(T)$ is a temperature- (or cryogenic suction-) dependent creep parameter defined as follows:

$$\psi_T = \psi_o\left(1+\frac{\theta}{\theta_o}\right)^b \quad [20]$$

where $\psi_o$ is the creep parameter at the reference temperature ($\theta_o$, typically 1 ºC); $b$ is a material parameter relating the changes in creep parameter with changes in temperature. In Eq. 19, the negative sign is used to indicate that the specific volume decreases with time. In Eq. 19, $t = 0$ corresponds to the end of the primary compression resulting in zero thermal viscoplastic volume change ($\delta V_m^{\sigma Tvp} = 0$; and $V_m = V_{NCL}$). Hence, Eq. 19 can also be written in the form of:

$$V_m = V_{NCL} - \psi_T \ln\left(\frac{t_o+t}{t_o}\right). \quad [21]$$

The same equation is also employed by Kelln et al. (2008) for the creep behavior of unfrozen soils. In the variational format, Eq. 19 can be written as:

$$\delta V_m^{\sigma Tvp} = -\frac{\psi_T}{t_o+t}\,\delta t \quad [22]$$

and one may obtain the thermal viscoplastic volumetric strain rate as:

$$\dot{\varepsilon}_p^{\sigma Tvp} = \frac{\delta \varepsilon_p^{\sigma Tvp}}{\delta t} = \frac{\delta V_m^{\sigma Tvp}/V_m}{\delta t} = \frac{\psi_T}{V_m\,(t_o+t)} \quad [23]$$

$\varepsilon_p^{\sigma Tvp}$ is considered to be positive in compression. Eq. 23 defines creep rate for an elapsed time $t$.

At time $t$ after primary compression, isotropically compressed states $p_m^* - V_m$ of the frozen soil can be defined in $\ln p^* - V$ plane by a line. This line is parallel to and at constant vertical $\delta V_m^{\sigma Tvp}$ separation from the NCL for the current frozen state of the soil. As the elapsed time for thermal viscoplastic straining approaches infinity, these states are defined by a line bounding further creeping. In unfrozen soils, Kelln et al. (2008) referred to this line as the viscoplastic limit line (VPL) (shown in Figure 2) where viscoplastic deformations cease. In frozen soils, depending on the ice content, temperature, and stress state of the soil, secondary creep can be followed by a tertiary creep with an accelerating creep rate. Under such conditions, the frozen soil is expected to fail over a shorter period of time than theoretical infinity. Hence, the termination of creeping may seem peculiar. Accordingly, the definition of the VPL for frozen soil is still necessary for the completeness of the mathematical description of the model. It should be noted that the location of the VPL does not significantly impact the magnitude of thermal viscoplastic strain rates. It will only control the extent by which the response of the soil is entirely elastic (discussed later in the Yield Surface subsection). Noting the parallelism of the VPL with the NCL, the following equation can be employed for the VPL:

$$V_{VPL} = Z - \lambda_f \ln p^* \quad [24]$$

where $Z$ is the intercept of the VPL at unit pressure in the current frozen state of the soil. At infinite time ($t = \infty$), in which the isotropic specific volume is on the VPL, the vertical separation between the VPL and NCL can be determined as $N_f - Z$.

The specific volume of the frozen soil at a specific time, say $t$, after primary compression can be stated by substituting Eq. 17 into Eq. 21 as follows:

$$V_m = N_f - \lambda_f \ln p_m^* - \psi_T \ln\left(\frac{t_o+t}{t_o}\right) \quad [25]$$

and then solving Eq. 25 for time $t$ results in

$$t = -t_o + t_o \exp\left(\frac{N_f - V_m}{\psi_T}\right)(p_m^*)^{-\frac{\lambda_f}{\psi_T}} \quad [26]$$

Replacing Eq. 26 into Eq. 23 gives the thermal viscoplastic volumetric strain rate for an isotropically compressed soil in the current frozen state as follows:

$$\dot{\varepsilon}_p^{\sigma Tvp} = \frac{\psi_T}{V_m\,t_o}\exp\left(\frac{V_m - N_f}{\psi_T}\right)(p_m^*)^{\frac{\lambda_f}{\psi_T}} \quad [27]$$

### 3.2.3. Yield Surface

A yield surface that is composed of a series of yield loci (YI) should be incorporated into the model to separate purely thermal elastic deformations of the frozen soil from thermal viscoplastic deformations. For this purpose, as briefly noted before, a yield surface with a similar shape to the PPS is adopted in the model according to the isotropic stress state corresponding to the current frozen state of the soil (see the yield locus associated with the isotropic stress state at AA, $YI_{AA}$, in Figure 2). Hence, the yield surface is expressed as follows:

$$F_Y = q^{*2} - M^2(p^* - \chi_t)(\chi - p^*) = 0 \quad [28]$$

in which $\chi$ $(= p_{f_Y}^*)$ and $\chi_t$ $(= p_{t_Y}^*)$ represent yielding in isotropic compression and in isotropic tension, indicating the size of the yield locus at the current frozen state of the soil ($S = S_1$) (see Figure 2). As shown in Figure 2, an isotropically compressed frozen soil under constant stress state creeps from AA on the NCL with increasing time to B and then to C. Thermal viscoplastic volumetric straining is associated with hardening of the soil and subsequently with the expansion of the yield locus. It can be assumed that the yielding criterion in isotropic compression ($p_{f_Y}^*$) is fixed

along the VPL in the compression plane. Thus, the intersection of the VPL (Eq. 24) with the unloading-reloading line (URL) corresponding to the initial yield locus gives the size of the initial yield locus in isotropic compression ($p^*_{f_Y}$) as follows:

$$p^*_{f_Y} = \exp\left[\left(\frac{1}{\lambda_f - \kappa_f}\right)(Z - V - \kappa_f \ln p^*)\right] \quad [29]$$

For the state $p^*_m - V_m$ of the frozen soil at AA in Figure 2, Eq. 29 gives the size of the initial yield locus (i.e., $p^*_{f_{Y_{AA}}}$). The isotropic hardening under the development of thermal viscoplastic volumetric strain increment can then be formulated in the hardening law as follows:

$$\delta p^*_{f_Y} = \left(\frac{V}{\lambda_f - \kappa_f} p^*_{f_Y}\right) \delta\varepsilon_p^{\sigma Tvp} \quad [30]$$

The yielding criterion in isotropic tension ($p^*_{t_Y}$), can be determined by the product of the ratio of $p^*_{f_{PPS}}/p^*_{f_Y}$ and $p^*_{t_{PPS}}$ ($= -k_t S_1$). Thermal creeping of frozen soil can now be associated with the expansion of the yield locus from AA ($Yl_{AA}$) to B ($Yl_B$) and then to C ($Yl_C$) (see Figure 2). The yield locus at the VPL where $V_m = V_{VPL}$, has reached the PPS that corresponds to the yield locus at C ($Yl_C = PPS_{A,B,C}$).

### 3.2.4. Flow Rule

So far, the model is formulated for an isotropic compression stress state corresponding to the current general stress state. In order to generalize the model to any loading path and stress state, a flow rule is required to relate plastic deformations to the current stress state. For this purpose, a non-associated flow rule is defined as:

$$\dot{\varepsilon}_{ij}^{\sigma Tvp} = \Lambda \frac{\partial F_{PPS}}{\partial \sigma^*_{ij}} \quad [31]$$

where $\Lambda$ is a scaler multiplier; $F_{PPS}$ stands for the PPS passing through the current stress state defined as follows:

$$F_{PPS} = {q^*}^2 - M^2(p^* - \xi_t)(\xi - p^*) = 0 \quad [32]$$

in which $\xi$ ($= p^*_m = p^*_{f_{PPS}}$) and $\xi_t$ ($= p^*_{t_{PPS}}$) are the parameters used to indicate the size of the plastic potential at the current stress state ($q^* - p^* - S_1$) (see Figure 2). Given the assumption that the thermal viscoplastic volumetric strain increment (or rate) is constant on the plastic potential (see A and AA in Figure 2), the plastic multiplier can be determined as the quotient of $\varepsilon_p^{\sigma Tvp}$ (Eq. 27) and $\partial F_{PPS}/\partial p^*$:

$$\Lambda = \frac{\psi_T}{V_m\, t_o} \exp\left(\frac{V_m - N_f}{\psi_T}\right) (p^*_m)^{\frac{\lambda_f}{\psi_T}} \frac{1}{|\partial F_{PPS}/\partial p^*|} \quad [33]$$

Substituting Eq. 33 into Eq. 31 gives the expression for the thermal viscoplastic strain rates in a general stress state:

$$\dot{\varepsilon}_{ij}^{\sigma Tvp} = \frac{\psi_T}{V_m\, t_o} \exp\left(\frac{V_m - N_f}{\psi_T}\right) (p^*_m)^{\frac{\lambda_f}{\psi_T}} \frac{1}{|\partial F_{PPS}/\partial p^*|} \frac{\partial F_{PPS}}{\partial \sigma^*_{ij}} \quad [34]$$

The thermal elastic-viscoplastic stress-strain response of the frozen soil is now completed and can be determined as:

$$\dot{\varepsilon}_{ij} = \frac{\dot{p}^*}{3K_{eq}} \delta_{ij} + \frac{1}{2G_{eq}} \dot{s}^*_{ij} + \dot{\varepsilon}_{ij}^{\sigma Tvp} + \dot{\varepsilon}_{ij}^{suc} \quad [35]$$

Eq. 35 reveals that strain increments can be developed by changes in solid phase stress and/or cryogenic suction (or temperature). In addition, in a constant stress state $\sigma^*_{ij}$ and $S$, time-dependent (i.e., viscoplastic) strain increments can still be developed at the frozen state of the soil due to the time increment. Also, in a constant solid phase stress state ($\sigma^*_{ij}$), changes in temperature rate (or cryogenic suction rate) cause temperature- and time-dependent (i.e., thermal viscoplastic) strain increments.

## 4 DETERMINATION OF MODEL PARAMETERS

In order to investigate the rate-dependent behavior of the frozen soils within the proposed TEVP constitutive model, 18 parameters, in total, are required to be determined. Ten parameters are required for describing the behavior under the variation of the solid phase stress ($G_{uf}$, $E_{uf}$, $a$, $\nu_f$, $p^*_o$, $p^*_r$, $\lambda_o$, $\kappa_o$, $N_o$, $M$); one parameter for calculating cryogenic suction-induced strain rates ($\kappa_s$); three parameters for coupling effects ($\alpha$, $\beta$, $k_t$); and four parameters for describing rate effects ($\psi_o$, $b$, $t_o$, $Z$). Table 1 presents the experimental tests proposed to determine these parameters.

Table 1. Proposed tests to determine the TEVP model parameters

| | Test | Sample | | Parameter |
|---|---|---|---|---|
| | | State | Temp (°C) | |
| 1 | Isotropic drained compression | Unfrozen | 0 | $(\lambda_o, \kappa_o, N_o, p^*_o, p^*_r)$ |
| 2 | Drained shear stress | | 0 | $(G_{uf}, M)$ |
| 3 | Unconfined triaxial compression | | 0 | $(E_{uf})$ |
| 4 | Unconfined triaxial compression | Frozen | At different negative temperatures | $(a)$ |
| 5 | Isotropic compression | | At any specific ice saturation | $(\nu_f)$ |
| 6 | Isotropic compression | | At two different temperatures | $(\alpha, \beta)$ |
| 7 | Drained shear stress | | At any negative temperature | $(k_t)$ |
| 8 | Freezing-thawing cycling | | Between two different temperatures | $(\kappa_s)$ |
| 9 | Creep | | At different negative temperatures | $(\psi_o, b, t_o, Z)$ |

## 5 MODEL DEMONSTRATION

In this section, the model predictions of time- and temperature-dependent behavior of frozen soils are compared with those of the two sets of experimental tests from the literature to examine its ability and accuracy. For this purpose, the results of triaxial compression tests and uniaxial creep tests conducted on frozen soils are reproduced.

### 5.1 Triaxial Compression Tests (TCTs)

A number of triaxial compression tests at different temperatures were performed by Xu (2014) on frozen sand samples. Due to the rapid freezing, ice lensing was avoided. The tests were conducted at a constant axial strain rate of $1.67\times10^{-4}$ $s^{-1}$ and initial confinement of 1 MPa. The values of cryogenic suction corresponding to the test temperatures are calculated using Eq. 4. The material parameters used for the simulations are listed in Table 2. Figure 3 compares the predictions of the TEVP model and experimental test results.

Table 2. Model parameters used in the simulation of TCTs and UCTs

| Parameter | Unit | Value | |
|---|---|---|---|
| | | TCTs | UCTs |
| $G_{uf}$[1] | kPa | 3500 | 5000 |
| $E_{uf}$ | kPa | $200\times10^3$ | $140\times10^3$ |
| $\kappa_o$[1] | --- | 0.08 | 0.01 |
| $\lambda_o$[1] | --- | 0.85 | 0.02 |
| $N_o$ | --- | 8.6 | 1.62 |
| $p_o^*$[1] | kPa | 5550 | 280 |
| $p_r^*$[1] | kPa | 100 | 50 |
| $M$[1] | --- | 1.5 | 0.85 |
| $a$ | --- | 0.4 | 0.07 |
| $\nu_f$[1] | --- | 0.31 | 0.48 |
| $\alpha$[1] | --- | 0.66 | 0.49 |
| $\beta$[1] | $kPa^{-1}$ | 0.00011 | 0.00015 |
| $k_t$ | --- | 0.1 | 0.45 |
| $\kappa_s$[1] | --- | 0.008 | 0.008 |
| $\psi_o$ | --- | 0.02 | 0.001 |
| $b$ | --- | 0.3 | 0.4 |
| $t_o$ | min | 1440 | 1 |
| $Z$ | --- | 1 | 1 |

[1] The values of this parameter are adopted from Ghoreishian Amiri et al. (2016a).

### 5.2 Uniaxial Creep Tests (UCTs)

Eckardt (1979) investigated the stress-strain behavior of frozen sand samples under different negative temperatures and creep stresses by conducting uniaxial creep tests. The creep deformation of the frozen soil at two temperatures (-5 and -15 ˚C) and four creep stresses (1, 3, 5, and 6 MPa) are reproduced within the formulation of the TEVP model. The material properties for these simulations are provided in Table 2. The predictions of the TEVP model for four of these tests are plotted and compared with those of the tests in Figure 4. Solid lines denote the model results.

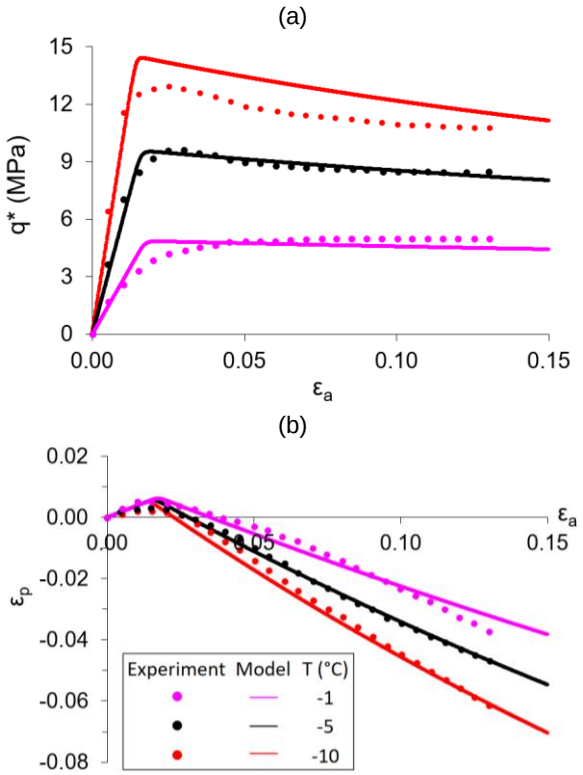


Figure 3. Triaxial compression tests on frozen sand at different temperatures: (a) deviatoric stress-axial strain ($q^* - \varepsilon_a$) plot; (b) volumetric strain-axial strain ($\varepsilon_p - \varepsilon_a$) plot.

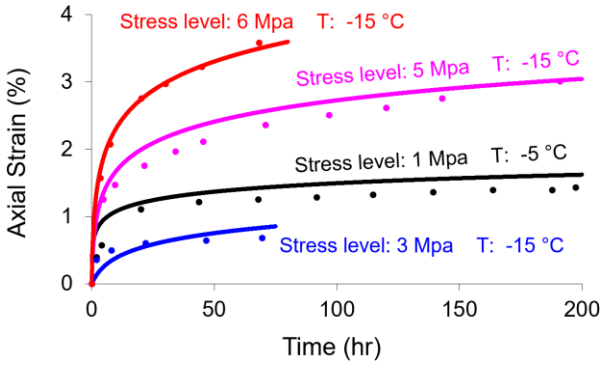


Figure 4. Uniaxial creep tests on frozen sand: axial strain-time plot.

As shown in Figures 3 and 4, the TEVP model can satisfactorily predict the behavior of frozen soils under different temperatures and confining stress.

## 6 CONCLUSION

A thermal elastic-viscoplastic constitutive model based on the framework of Critical State Soil Mechanics was proposed to examine the rate-dependent behavior of frozen soils. The model was formulated within the two stress-state variables framework where the cryogenic suction and solid phase stress were considered as the independent stress variables. A logarithmic creep function was adopted to represent time- and temperature-dependent plastic deformations of frozen soils. Plastic potential and yield surfaces were defined based on the current stress state of the soil. The hardening (softening) of the soil was formulated based on the definition of the viscoplastic limit line. The capability of the model was examined by reproducing the conventional triaxial compression and creep tests results. The model can also simulate the impacts of temperature change rate so that it can be used to investigate the behavior of the frozen ground under extreme short-term as well as long-term climatic events in permafrost regions.

## 7 REFERENCES


Teufel, B. and Sushama, L. 2019. Abrupt changes across the arctic permafrost region endanger northern development. *Nature Climate Change*, 9 (11), 858–862.

Andersland, O. B. and Ladanyi, B., 2003. *Frozen ground engineering*. John Wiley & Sons.

Vyalov, S. 1986. *Rheological Fundamentals of Soil Mechanics*. Elsevier, Amsterdam.

Arenson, L. U., & Springman, S. M. 2005. Triaxial constant stress and constant strain rate tests on ice-rich permafrost samples. *Canadian Geotechnical Journal*, 42(2), 412–430.

Yao, X., Xu, G., Zhang, M., and Yu, F. 2019. A frozen soil rate dependent model with time related parabolic strength envelope. *Cold Regions Science and Technology*, 159, 40–46.

Ghoreishian Amiri, S. A., Grimstad, G. and Kadivar, M. 2016a. An elastic-viscoplastic model for saturated frozen soils. *European Journal of Environmental and Civil Engineering*, 1–17.

Perzyna, P., 1963. The constitutive equations for rate sensitive plastic materials. *Quarterly of Applied Mathematics*, 20 (4), 321–332.

Sun, Y., Weng, X., Wang, W., Niu, H., Li, H. and Zhou, R. 2021. A thermodynamically consistent framework for visco-elasto-plastic creep and anisotropic damage in saturated frozen soils. *Continuum Mechanics and Thermodynamics*, 33 (1), 53–68.

Li, B., Zhu, Z., Ning, J., Li, T. and Zhou, Z. 2022. Viscoelastic–plastic constitutive model with damage of frozen soil under impact loading and freeze–thaw loading. *International Journal of Mechanical Sciences*, 214, 106890.

Nishimura, S, Gens, A., Olivella, S., and Jardine, R. 2009. THM-coupled finite element analysis of frozen soil: Formulation and application. *Géotechnique*, 59(3), 159–171.

Ghoreishian Amiri, S., Grimstad, G., Kadivar, M. and Nordal, S. 2016b. Constitutive model for rate-independent behavior of saturated frozen soils. *Canadian Geotechnical Journal*, 53(10), 1646–1657.

Rempel, A. W., Wettlaufer, J., and Worster, M. G. 2004. Premelting dynamics in a continuum model of frost heave. *Fluid Mechanics*, 498, 227–244.

Alonso, E. E., Gens, A., and Josa, A. 1990. A constitutive model for partially saturated soils. *Géotechnique*, 40(3), 405–430.

Tavenas, F, Leroueil, S, Rochelle, P. L., and Roy, M. 1978. Creep behaviour of an undisturbed lightly overconsolidated clay. *Canadian Geotechnical Journal*, 15(3), 402–423.

Kelln, C. G., Sharma, J., Hughes, D., and Graham, J. 2008. An improved elastic–viscoplastic soil model. *Canadian Geotechnical Journal*, 45(10), 1356–1376.

Yin, J.-H., and Graham, J. 1999. Elastic viscoplastic modelling of time-dependent stress–strain behavior of soils. *Canadian Geotechnical Journal*, 36: 736–745.

Xu, G. 2014. Hypoplastic constitutive models for frozen soil (Doctoral dissertation). University of Natural *Resources and Life Sciences,* Vienna, Austria.

Eckardt, H. 1979. Creep behaviour of frozen soils in uniaxial compression tests. *Engineering Geology*, 13(1), 185-195.